Supplementary Information

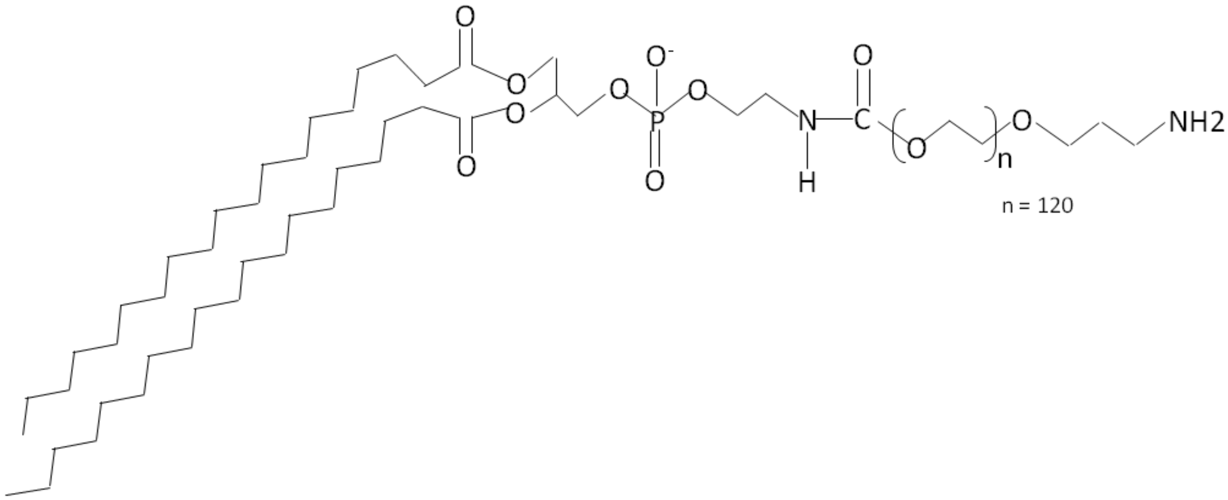

Figure 1: Molecular structure of the PL-PEG used in the experiments. The simulated DSPE-PEG-NH_2 structures contain 45 or 120 PEG monomers.

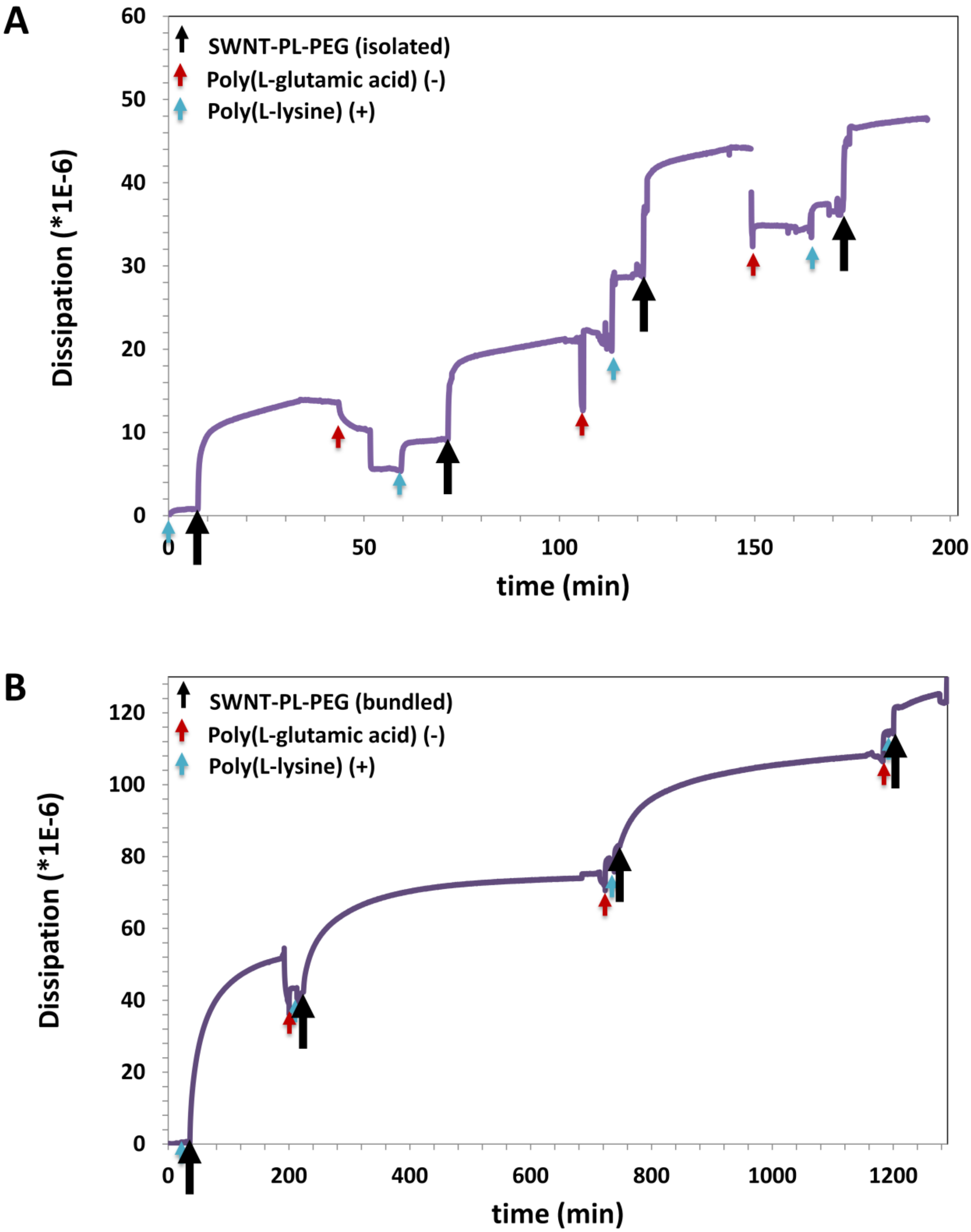

Figure 2: Quartz crystal microgravimetry with dissipation (QCMD) sensograms of resonator dissipation factor versus time, during layer-by-layer assembly of SWNT-PL-PEG with poly(L-lysine) and poly(L-glutamic acid), for cases of isolated (A) and bundled (B) SWNT.

The MARTINI coarse-grained (CG) models of PL-PEG and CNT.

To generate the model for the aqueous phospholipid poly(ethylene glycol) (PL-PEG) / carbon nanotube (CNT) system, we choose the framework of the MARTINI CG force-field.[1,2] The MARTINI force-field was originally developed for lipids and detergents[1,2], but later extended to proteins[3], lipoproteins[4], fullerenes[5,6], graphene[7] and CNT[8]. In the MARTINI model, the atoms of a molecule are replaced with specific interaction centers: on average one interaction center consists of four non-hydrogen atoms. Interaction sites are categorized into four different main types: charged, polar, nonpolar, and apolar, and within these groups to subtypes based on, for example, polarity or hydrogen-bonding capabilities. The viability of the MARTINI CG approach for polymers has been tested for biopolymers, such as PL-PEG[9, 10], as well as synthetic polymers such as polystyrene[11, 12]. The molecular level CG modeling based scheme is chosen because compared to fully atomistic models, it allows for larger systems and longer timescales to be studied with the same computational effort. The speed up is mainly due to the CG approach smoothing out the interaction potential enabling the use of a longer time-step. Additionally, due to the smoothing of the interaction potential, the CG simulation time corresponds to a significantly longer actual time. For MARTINI, a factor of 4 based on, *e.g.*, diffusion rates is typically used in converting the simulation time to real time.[1, 13] In this work all simulation times are converted.

Models.

We choose DSPE-PEG-NH_2 (IUPAC name (aminopropyl polyethyleneglycol)carbamyl-distearoylphosphatidyl-ethanolamine) as the PL-PEG in compliance with the experiments. The model for DSPE-PEG-NH_2 is constructed by modifying the standard MARTINI DSPE lipid[1] to include the MARTINI PEG tail, introduced and thoroughly verified in Ref. [14], and the final capping NH_2 group described by MARTINI SNd bead type, thus obtaining the model for the PL-PEG.

The MARTINI PEG model has been thoroughly validated against experimental and all-atom simulation data on diffusivities, hydrodynamics, end-to-end-distances, bond lengths, angles, and dihedrals[14]. Similarly combined with a MARTINI phospholipid, the PEG model has accurately reproduced experimental data of PL-PEG aggregates in Refs.[9,10,14]. For representing the NH_2 group, the Nd bead type parameterized for 1-propylamine[1], is chosen over other MARTINI bead possibilities due to correctly described proportional interactions with the lipid end of the PL-PEG molecule. Furthermore, to obtain consistently scaled Lennard-Jones interactions with the PEG-PEG tail[14], the SNd version of the Nd bead is used.

CG single walled carbon nanotube (SWNT) models are developed representing atomistic (10,0) SWNT with a diameter of ~0.8 nm. CG SWNT are described by a 3-to-1 mapping, effectively a CG (5,0) tube with effective bead-bead distance of 2.84 Å instead of the atomistic 1.42 Å carbon-carbon separation. This CG model preserves SWNT chirality and symmetry. The interaction model and the force constants of the SWNT beads are described in Ref. [15]. Due to the large radius of curvature in a (5,0) CG tube, the SWNT bead distances are further constrained by the Lincs algorithm[16]. For water and counter-ions, standard MARTINI water and ion beads are used[1].

Simulation Protocols.

Simulations are performed in the NPT ensemble using the GROMACS 4.5.5 simulation package[17,18]. For thermostating, the stochastic velocity rescaling thermostat of Bussi et al. is employed[19] with temperature T=298K. A pressure of 1 bar is maintained with the Parrinello-Rahman pressure control[20] using τ_p = 4 ps semi-isotropically with the SWNT axial direction pressure controlled separately. A cut-off of 1.2 nm is employed for the Lennard-Jones (LJ) potential and electrostatic interactions. The LJ interactions are shifted to zero smoothly between 0.9 nm and 1.2 nm, and the Coulombic interactions between 0 nm and 1.2 nm. A time step of 8 ns is used to be consistent with the PL-PEG simulations of Lee *et al.* [9, 14, 15]. With the exception of a somewhat shorter time-step (typically 10 fs), the simulation protocol corresponds to the standard MARTINI protocol.

Systems.

PL-PEG concentrations of 0.12 and 0.19 v/w is considered with a single SWNT and a bundle of 7 SWNT (diameter ~3.2 nm). PEG lengths of 45 and 120 monomers are considered, corresponding to molecular weights 3000 and 6400, respectively. An isolated SWNT is modeled as a 20 nm long CG SWNT of diameter 0.8 nm, spanning the periodic simulation box. A SWNT bundle consists of 7 identical SWNT in regular hexagonal packing.

SWNT or a bundle of 7 SWNT are initially solvated with ~50000 CG water molecules in a periodic box of size (20,20,20) nm^3. To fully coat the SWNT with a PL-PEG layer, 300 PL-PEG molecules v/w 0.19 with a PEG chain length of 45 monomers and their respective sodium counterions are inserted randomly into the simulation box. To prevent the CG water from artificial freezing, which may happen when there are large nucleation sites present, roughly 2 percent of water particles are converted into antifreeze water beads WF.[1, 2] For assessing the effect of concentration, 100 PL-PEG molecules farthest away from the SWNT or bundle are removed from the 0.19 v/w configuration at 1.44 µs and replaced with water beads, thus making the total number of PL-PEG 200, corresponding to v/w 0.12. These simulations are run for 2.24 µs (isolated SWNT) and 2.08 µs (bundled SWNT) for the v/w 0.12 concentration, and 2.4 µs (isolated SWNT), and 2.40 µs (bundled SWNT) for the v/w 0.19 concentration.

Finally, to probe the effect of the PEG chain length, simulations with a single SWNT and a bundle of 7 SWNT with 200 PL-PEG molecules of 120 monomer PEG chains (M_w = 6400) are constructed. The PL-PEG concentration is maintained at 0.12 v/w (simulation box size (30, 30, 20) nm^3). The PL-PEG-SWNT complexes are simulated in vacuo for 8 ns to speed up the micellization dynamics. The resulting aggregates are then solvated with ~130000 CG waters (520 000 atomic waters) with again ~2% antifreeze waters. We note that for comparison purposes, in all the simulations the dimension corresponding to the SWNT axial length remains the same, and the v/w ratio is matched between the systems with different PL-PEG tail lengths. These comparison simulations are run for 2.24 μs (isolated SWNT) and 1.76 μs (bundled SWNT). The computational cost of longer simulations is prohibitive.

Initial relaxation.

All simulations begin by first setting the compressibility to zero in the SWNT axial direction to prevent the bending of the SWNT structure. A short simulation of few ns is then run to ensure that the pressure is equilibrated, after which the semi-isotropic pressure coupling is enabled allowing for also the SWNT axial direction to equilibrate. The first 400 ns in all simulations are omitted in the data analysis.

Data analysis.

The diameter of the hydrophobic core of the PL-PEG micelles is calculated by determining the radius of gyration of the hydrophobic part of each PL-PEG micelle in the solution (*i.e.* the lipid tail and the glycerol beads of the PL-PEG molecules in the micelle). The PL-PEG bound on the SWNT surface are excluded in this calculation. Throughout, any PL within 1 nm of the surface is classified as bound. The total hydrophobic core diameter reported is twice the average of the hydrophobic radius of gyration (R_g) over all micelles.

The PL-PEG density on the SWNT or the bundle surface is calculated with respect to the surface accessible area, *i.e.,* the calculation takes into account the excluded volume effects. For calculating the excluded volume, the graphene-graphene equilibrium separation distance 0.3 nm is used as an approximation of the minimum distance between a particle and the SWNT surface. Again, the PL-PEG molecules are considered bound to the SWNT or the SWNT bundle if the PL part is within 1 nm of the surface.

The PL-PEG chain extension is evaluated by calculating the average radius of gyration $\langle R_g \rangle$ value of the bound PL-PEG molecules (per molecule).

1 Marrink, S. J.; Risselada, H. J.; Yefimov, S.; Tieleman, D. P.; de Vries, A. H. *J. Phys. Chem. B* **2007,** *111,* 7812–7824.

2 Marrink, S. J.; de Vries, A. H.; Mark, A. E. *J. Phys. Chem. B* **2003,** *108,* 750–760.

3 Monticelli, L.; Kandasamy, S. K.; Periole, X.; Larson, R. G.; Tieleman, D. P.; Marrink, S.-J. *J. Chem. Theory Comput.* **2008,** *4,* 819–834.

4 Catte, A.; Patterson, J. C.; Bashtovyy, D.; Jones, M. K.; Gu, F.; Li, L.; Rampioni, A.; Sengupta, D.; Vuorela, T.; Niemelä, P.; Karttunen, M.; Marrink, S. J. J.; Vattulainen, I.; Segrest, J. P. *Biophysical journal* **2008,** *94,* 2306–2319.

5 Wong-Ekkabut, J.; Baoukina, S.; Triampo, W.; Tang, I.-M. M.; Tieleman, D. P.; Monticelli, L. *Nature nanotechnology* **2008,** *3,* 363–368.

6 Monticelli, L. *J. Chem. Theory Comput.* **2012,** *8,* 1370–1378.

7 Titov, A. V.; KraÌl, P.; Pearson, R. *ACS Nano* **2009,** *4,* 229–234.

8 Wallace, E. J.; Sansom, M. S. *Nano letters* **2007,** *7,* 1923–1928.

9 Lee, H.; Pastor, R. W. *The journal of physical chemistry. B* **2011,** *115,* 7830–7837.

10 Yang, S.-C.; Faller, R. *Langmuir* **2011,** *28,* 2275–2280.

11 Rossi, G.; Giannakopoulos, I.; Monticelli, L.; Rostedt, N. K. J.; Puisto, S. R.; Lowe, C.; Taylor, A. C.; Vattulainen, I.; Ala-Nissila, T. *Macromolecules* **2011,** *44,* 6198–6208.

12 Rossi, G.; Monticelli, L.; Puisto, S. R.; Vattulainen, I.; Ala-Nissila, T. *Soft Matter* **2011,** *7,* 698–708

13 Baron, R; Trzesniak, D; de Vries, A. H.; Elsener, A; Marrink, S. J.; van Gunsteren, W.F. *ChemPhysChem*, 2007, 8, 452–461

14 Lee, H.; de Vries, A. H.; Marrink, S.-J.; Pastor, R. W. *J. Phys. Chem. B* **2009,** *113,* 13186–13194.

15 Lee, H. ; Kim, H; *The journal of physical chemistry. C*, 2012, **116** (16), pp 9327–9333

16 Hess, B.; Bekker, H.; Berendsen, H. J. C.; Fraaije, J. G. E. M. *J. Comput. Chem.* **1997,** *18,* 1463–1472.

17 Hess, B.; Kutzner, C.; van der Spoel, D.; Lindahl, E. *J. Chem. Theory Comput.* **2008,** *4,* 435–447.

18 Van Der Spoel, D.; Lindahl, E.; Hess, B.; Groenhof, G.; Mark, A. E.; Berendsen, H. J. *Journal of computational chemistry* **2005,** *26,* 1701–1718.

19 Bussi, G.; Donadio, D.; Parrinello, M. *The Journal of Chemical Physics* **2007,** *126,* 014101+.

20 Parrinello, M.; Rahman, A. *Journal of Applied Physics* **1981,** *52,* 7182–7190.